Natural Resources Canada
Ressources naturelles Canada

Geophysical modelling of the Neoarchean Woodburn Lake and Paleoproterozoic Ketyet River groups, and plutonic rocks in central Schultz Lake map area, Nunavut

P.A. Tschirhart, W.A. Morris, and C.W. Jefferson

Geological Survey of Canada
Current Research 2013-2

2013

Canada

Geological Survey of Canada
Current Research 2013-2

Geophysical modelling of the Neoarchean Woodburn Lake and Paleoproterozoic Ketyet River groups, and plutonic rocks in central Schultz Lake map area, Nunavut

P.A. Tschirhart, W.A. Morris, and C.W. Jefferson

2013

ISSN 1701-4387
Catalogue No. M44-2013/2E-PDF
ISBN 978-1-100-21526-6
doi:10.4095/292116

A copy of this publication is also available for reference in depository libraries across Canada through access to the Depository Services Program's Web site at http://dsp-psd.pwgsc.gc.ca

This publication is available for free download through GEOSCAN http://geoscan.ess.nrcan.gc.ca

Recommended citation

Tschirhart, P.A., Morris, W.A., and Jefferson, C.W., 2013. Geophysical modelling of the Neoarchean Woodburn Lake and Paleoproterozoic Ketyet River groups, and plutonic rocks in central Schultz Lake map area, Nunavut, 19 p. doi:10.4095/292116

Critical review

P. Keating

Authors

P.A. Tschirhart (tschirpa@mcmaster.ca)
W.A. Morris (morriswa@mcmaster.ca)
McMaster Applied Geophysics and Geological Imaging Centre
School of Geography and Earth Sciences
McMaster University
Hamilton, Ontario L8S 4K1

C.W. Jefferson (Charlie.Jefferson@NRCan-RNCan.gc.ca)
Geological Survey of Canada
601 Booth Street
Ottawa, Ontario K1A 0E8

Correction date:

Geophysical modelling of the Neoarchean Woodburn Lake and Paleoproterozoic Ketyet River groups, and plutonic rocks in central Schultz Lake map area, Nunavut

P.A. Tschirhart, W.A. Morris, and C.W. Jefferson

Tschirhart, P.A., Morris, W.A., and Jefferson, C.W., 2013. Geophysical modelling of the Neoarchean Woodburn Lake and Paleoproterozoic Ketyet River groups, and plutonic rocks in central Schultz Lake map area, Nunavut, 19 p. doi:10.4095/292116

Abstract: Uranium exploration in the Thelon Basin has been has been revitalized by developments and discoveries reported by AREVA Resources Canada and Cameco Corporation in structurally intercalated metasedimentary and metavolcanic rocks of the Neoarchean Woodburn Lake group and early Paleoproterozoic Ketyet River group south and east of the Aberdeen Subbasin. This study integrates geophysics and geology to model a proposed basement klippe located south of Schultz Lake in central NTS map area 66A.

Orthogonal high-resolution ground gravity transects were acquired in 2010, based on initial definition of the structure by a published 2004 geological map. These were integrated with high-resolution aeromagnetic and electromagnetic data from Forum Uranium Corporation, CanVec topographic data, and initial detailed geological observations in 2010 to 2011 by parallel studies under the Northern Uranium for Canada Project, part of the Geomapping for Energy and Minerals (GEM) Program

The subsurface geology was computed by integrating surface geological contacts, unconstrained geophysical inversions and forward models. The unconstrained magnetic inversions defined several dyke arrays and suggest a deep seated mafic-to-felsic pluton tentatively assigned to the 2.6 Ga Snow Island Suite. High-resolution electromagnetic data provide strong constraints on near-surface lithology and steeply dipping faults, discriminating between Paleoproterozoic quartzite, Paleoproterozoic grey schist, and Neoarchean arkosic metagreywacke. The forward models, primarily constrained by generic rock properties and the clear gravity signal, support the klippe hypothesis. Further improvement could be achieved with a detailed gravity grid and more site-specific rock properties, and through collaborative integration and feed-back analysis of the full structural mapping data set.

Résumé : La prospection de l'uranium dans le bassin de Thelon a été relancée à la suite des travaux de mise valeur et des découvertes rapportés par la société AREVA Resources Canada et la Corporation Cameco dans les roches métasédimentaires et métavolcaniques structuralement intercalées du groupe de Woodburn Lake du Néoarchéen et du groupe de Ketyet River du Paléoprotérozoïque précoce, au sud et à l'est du sous-bassin d'Aberdeen. La présente étude intègre des données géophysiques et géologiques afin de modéliser une klippe du socle proposée, située au sud du lac Schultz dans le centre de la région cartographique 66A du SNRC.

En se fondant sur une carte géologique publiée en 2004 qui offrait une définition initiale de la klippe, des données de gravimétrie haute résolution ont été acquises au sol en 2010 le long de transects orthogonaux. L'information tirée de ces transects a été intégrée à des données aéromagnétiques et électromagnétiques haute résolution provenant de la Forum Uranium Corporation, à des données topographiques de CanVec et à des observations géologiques initiales détaillées, recueillies en 2010 et 2011 lors d'études menées en parallèle dans le cadre du projet Uranium du programme Géocartographie de l'énergie et des minéraux.

La géologie de subsurface a été reconstituée en intégrant l'information tirée des contacts géologiques en surface, d'inversions géophysiques sans contraintes et de modèles directs. Les inversions magnétiques sans contraintes ont permis de déterminer la présence de plusieurs essaims de dykes et laissent supposer l'existence en profondeur d'un pluton de composition mafique à felsique, qui appartient vraisemblablement à la Suite de Snow Island datant de 2,6 Ga. Les données électromagnétiques haute résolution fournissent de puissantes contraintes sur la lithologie près de la surface et les failles à fort pendage, nous permettant d'établir une distinction entre le quartzite du Protérozoïque, le schiste gris du Paléoprotérozoïque et la métagrauwacke arkosique du Néoarchéen. Les modèles directs, principalement encadrés par les propriétés génériques des roches, et un signal gravimétrique net soutiennent l'hypothèse d'une klippe. Des améliorations additionnelles pourraient être réalisées grâce au levé détaillé d'une grille gravimétrique et à l'obtention des propriétés lithologiques propres au site, ainsi que par une approche de collaboration fondée sur l'intégration du jeu complet de données issu de la cartographie structurale et l'analyse des rétroactions.

INTRODUCTION

The Thelon Basin, located west of Baker Lake, Nunavut, has in recent decades become a high priority target for uranium (U) exploration due to its potential to host world class grade U deposits (Fig. 1). The basin has many similarities (size, age, and geological attributes) to that of the world's highest concentration of U deposits, the Athabasca Basin, Saskatchewan. Both the Athabasca and Thelon basins host unconformity associated uranium deposits, with average deposit grades in the Thelon Basin being 0.4%, less than the approximately 2% for the Athabasca Basin, but significantly higher than the 0.03% at the world's largest single U deposit, Olympic Dam, Australia (Jefferson et al., 2007).

Exploration is most active and all major discoveries to date have been in basement rocks of the Woodburn Lake group along the southeastern edge of the northeastern part of Thelon Basin. The area of this study is a klippe mapped by Hadlari et al. (2004) south of Schultz Lake that is within a larger area staked by Forum Uranium Corporation, some 30 km east of a cluster of deposits here termed the Kiggavik camp (Fig. 1). This active area of uranium exploration includes development drilling of multiple known deposits by AREVA Resources Canada, three recent drill discoveries by Cameco Corporation, and several showings in Forum Uranium Corporation's claim area. Forum Uranium Corporation's klippe area has been shown from fieldwork during the summer of 2010 to have many geological elements in common with the Kiggavik camp, as outlined in section 'Geological setting' below.

The purpose of this study in general is to provide better constraints on the Neoarchean to early Paleoproterozoic basement complex in the klippe area, as part of a general strategy under the Geomapping for Energy and Minerals Program to improve framework knowledge for exploration here as well as extrapolated toward the west and beneath the Thelon Basin. Specific to the study area, the aim is to test the hypothesis that the main structure is a klippe of Ketyet River group structurally overlying the Woodburn Lake group. Outcrop within the klippe area is limited; a number of possible geometries can explain the observed lithological and structural data (McEwan, 2012). In this paper the authors attempt to model the subsurface geology through the integration of gravity, magnetic and electromagnetic (EM) data sets, preliminary geological maps, and field samples. Subsurface structure was interpreted using source edge detection on the EM data, visual analysis of satellite imagery, and unconstrained inversion of the aeromagnetic data. The subsurface interpretation was tested for consistency by modelling two detailed ground-gravity profiles. These models are not intended to be geologically balanced at this stage, but do invoke reasonable generalized geological configurations that may account for the observed geophysical signals and could be considered in developing balanced geological cross-sections.

GEOLOGICAL SETTING

Located in the northern Rae Domain of the Churchill Structural Province, the Thelon Basin is a remnant of a somewhat thicker and broader repository that is thought to have covered the study area, but is now preserved only to the north and west. The Barrensland Group filled the Thelon Basin and represents the upper 1–3 km of the Dubawnt Supergroup which was deposited after 1830 Ma as the result of strike-slip-extensional faulting during the late stages of, and following the Trans-Hudson Orogeny (Davis et al., 2011; Rainbird et al., 2010; Jefferson et al., 2011a, b). The Dubawnt Supergroup is overall flat lying and unmetamorphosed, but in places pervasively altered. It unconformably overlies earlier Paleoproterozoic and Archean basement rocks (Renac et al., 2002) and comprises three major groups (Rainbird et al., 2003). The Baker Lake Group fills a series of deep basins located south of Baker Lake. It is unconformably overlain in succession by the Wharton and Barrensland groups that progressively overlap the older basement toward the west. Variably thick zones of paleoweathered (Davis et al., 2011) and hydrothermally altered (Fuchs and Hilger, 1989) basement rocks underlie the basal conglomerate units of the Wharton and Barrensland groups.

As noted in the 'Introduction' section, the focus of this study is on a representative parts of the Woodburn Lake and Ketyet River groups in the Tehek-Marjorie belt — an informally named Neoarchean to early Paleoproterozoic basement supracrustal complex that unconformably underlies the Thelon Basin, hosts all significant uranium prospects in this area, and was previously termed the Whitehills belt (Pehrsson et al., 2010). The klippe study area exposes an intriguing part of Tehek-Marjorie belt and is not obscured by Thelon Basin cover strata, thereby providing an ideal representation of the belt for geophysical modelling. The main geological map units here are Neoarchean supracrustal rocks of the Woodburn Lake group (informal name), and early Paleoproterozoic siliciclastic, minor carbonate, and mafic volcanic rocks of the Ketyet River group (informal name) (Zaleski et al., 2000; Rainbird et al., 2010; Jefferson et al., 2011a, b; McEwan, 2012). The northeast-trending Tehek-Marjorie fold and thrust belt (Fig. 1) records four major deformations and the associated metamorphism ranges from lower greenschist to middle amphibolite facies. The earliest distinguishable deformation involved early Paleoproterozoic nappe tectonics that tectonically interleaved Pipedream assemblage arkosic metawacke of the Neoarchean Woodburn Lake group with quartz arenite (hereafter termed "quartzite") and grey schist of the early Paleoproterozoic Ketyet River group. The most visible map-scale structures are D_2 open to tight folds that predated the Dubawnt Supergroup. Current descriptions of the stratigraphy and structure of the Tehek-Marjorie belt provided by Pehrsson et al. (2010) and Jefferson et al. (2011a, b, in press) are not required for geophysical modelling of the klippe area; however, they do provide important new interpretations of legacy data such as reported

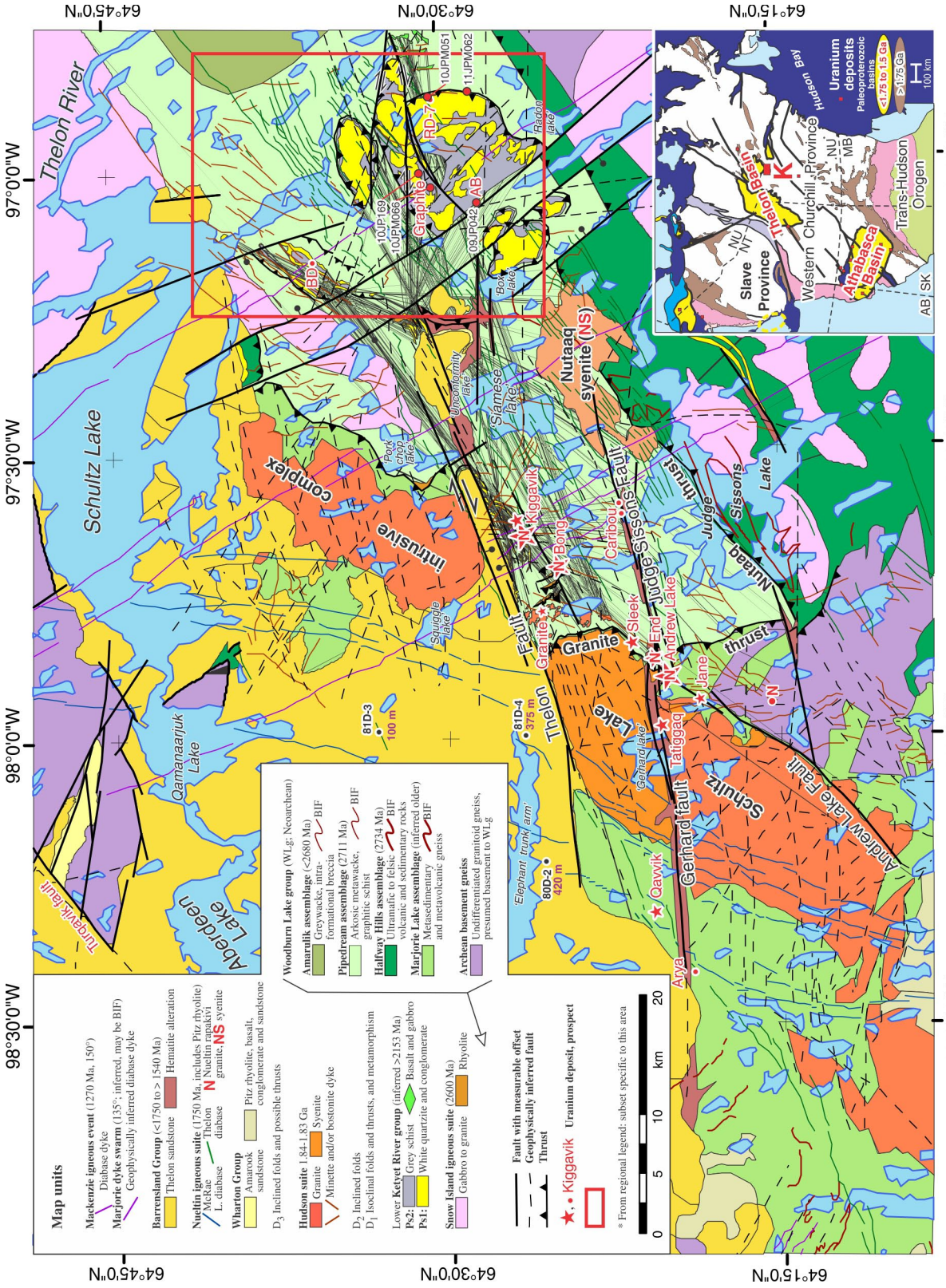

Figure 1. Regional geological context of the study area in the western part of the Tehek-Marjorie belt that encompasses the Kiggavik camp, southeast of the eastern Thelon Basin (*after* Jefferson et al. (in press), Fig. 2). Informal lake names are in single quotation marks to distinguish them from formal names. BIF = banded iron-formation.

by Zaleski et al. (2000), Hadlari et al. (2004), and Rainbird et al. (2010), and are currently being improved by integrating new data and concepts such as presented here. Hereafter, the informal term 'Pipedream metawacke' is used for that part of the Woodburn Lake group dominated by arkosic metagreywacke and graphitic schist, and 'Halfway Hills assemblage' for the denser, mafic metavolcanic-dominated part of the Neoarchean Woodburn Lake group.

A deep-seated granitoid pluton beneath the klippe is interpreted from a broad aeromagnetic high with gradational margins. Fieldwork in 2011 suggested that the 2.6 Ga pluton mapped by Hadlari et al. (2004) east of Judge Sisson's Lake is associated with the mafic phase of granitoid body with a similar, but much higher and broader magnetic anomaly. The interpreted deep-seated pluton of the klippe area is neither exposed, nor does it have any known metamorphic effects, but the assumption of it being a pluton is a fundamental underpinning to the geophysical modelling herein. A 30 m wide diabase dyke the intense linear aeromagnetic high of which discontinuously transects the klippe area at 155° is interpreted to be part of the continent-spanning 1.28 Ga (LeCheminant and Heaman, 1989) Mackenzie dyke swarm.

Generally undeformed, widely distributed midcrustal granitic to syenitic intrusions of the 1.85–1.8 Ga Hudson suite are important sheet-like crustal components in the Schultz Lake map area and are interpreted as a result of midcrustal melting, whereas the contemporaneous ultrapotassic low-silica volcanic rocks in the Baker Lake Basin reflect products of mantle melting. Diabase dykes trending about 010–025° and about 070–090°, represent the mafic trigger for rapakivi granite of the ca. 1.75 Ga Nueltin-suite (Scott et al., 2010, Scott, 2012; Peterson et al., 2010). These intrusions were contemporaneous with rhyolite and rare basalt of the Pitz Formation (T. Peterson, pers. comm., 2012), plus eolian to alluvial siliciclastic deposits, all part of the Wharton Group. The Thelon Basin was initiated at an unknown time after 1.75 Ga, bounded by arrays of faults trending parallel to the three above-mentioned dyke sets as well as several other trends, including reactivated curvilinear shear zones such as the about 060° Turqavik fault and about 080° Thelon fault array (Jefferson et al., 2011a, b; Tschirhart et al., 2011b). The last array of faults, some of which are occupied by the Thelon diabase dyke swarm, have right lateral offsets of up to 20 km or more and dip-slip offsets of tens of metres to hundreds of metres, north-side-down. In the klippe study area one strand of the Thelon fault array offsets a block of quartzite about 3 km right laterally with an unknown dip-slip component (Fig. 1). The Thelon Formation was cemented by uraniferous fluorapatite synchronous with faulting at ca. 1.67 Ga (Davis et al., 2011), and was capped by the ultrapotassic Kuungmi mafic volcanic rocks at ca 1.54 Ga (Chamberlain et al., 2010).

DATA FOR GEOPHYSICAL MODELLING

A number of different geological and geophysical data sets were obtained for this project. Gravity data were acquired during the 2010 field season along roughly perpendicular north-northwest–west-southwest lines, respectively, trending 335° for 30 km and 114° for 19 km (Fig. 2). Station spacing varies from 150 m to 500 m, being shorter across known or suspected geological contacts and relatively thin units. Data were collected to standards set and are managed by the Geodetic Survey Division of Natural Resources Canada. The digital geophysical data may be downloaded, at no charge, from Natural Resources Canada's Geoscience Data Repository for Geophysical and Geochemical data at http://gdr.nrcan.gc.ca. Elevations of gravity stations were determined by a Magellan Promark 3 differential GPS. Postprocessing of the field GPS data used GNSS solutions and GPS-H for Base-Receiver correlation and ellipsoidal correction respectively.

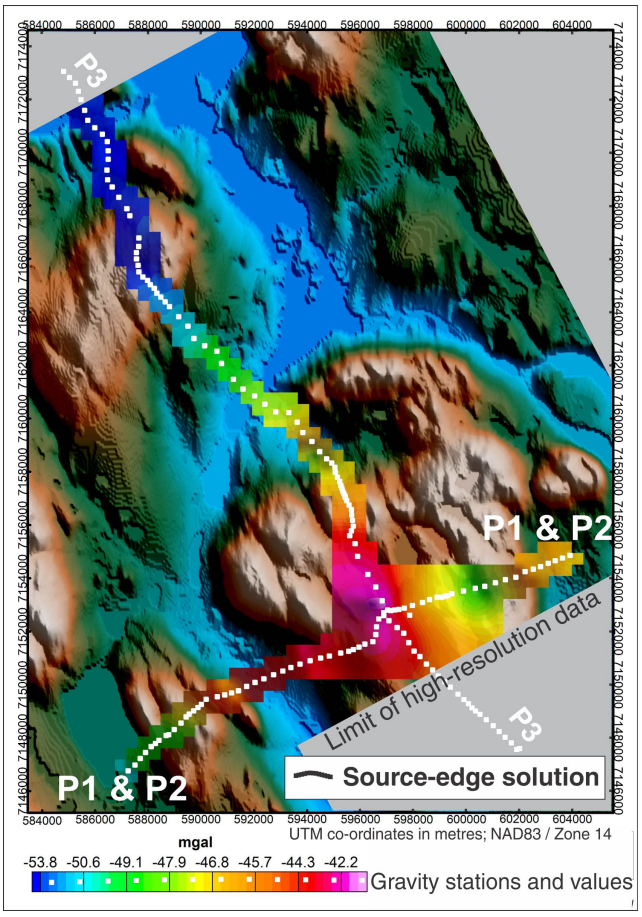

Figure 2. Complete Bouguer anomaly overlain on shaded digital elevation model (blue = low elevation, green-brown = moderate elevation, white = high elevation; artificial sun to the northeast). Gravity station locations (white squares) used in forward-gravity modelling are along lines from southwest to northeast (geophysical profiles P1 and P2 were made along this transect), and northwest to southeast (profile P3 was made from these data).

Gravity data were corrected for instrument drift, free-air, Bouguer anomaly and terrain using a density of 2.67 g/cm^3. Gravity data were then gridded to 200 m using the minimum curvature algorithm. As expected (Thomas and Wood, 2007), the complete Bouguer anomaly map (Fig. 2) is independent of topography.

Forum Uranium Corporation shared raw high-resolution total-magnetic-intensity (TMI) and electrical-conductivity data, as well as processed TMI and apparent resistivity (res) grids corresponding to frequencies 140 kHz, 40 kHz, 8200 Hz, 1800 Hz, and 400 Hz. Data for these grids were collected in 2008 by Fugro Airborne using their Resolve system at a flight height of 30 m and line spacing of 160 m. Data were gridded to 40 m cell size using the miniature curvature algorithm. The magnetic data are part of a compilation by Tschirhart et al. (2011a) and are publically available from the NRCan Geophysical Database.

Western Churchill Province residual total-field magnetic data were acquired from the NRCan Geophysical Database. These data were acquired in 1973 and 1974 at a mean terrain clearance of 300 m and a line spacing of 800 m. Flight lines were oriented east-west. Data were gridded to 400 m using the minimum curvature algorithm. As the data were coarse and noisy, they were microlevelled following the procedure described by Minty (1991) in order to remove directional noise not removed by the original levelling. The coarse resolution of this data set limited the interpretation of any geological features smaller than 1600 m in the north-south direction, but because the high-resolution magnetic data supplied by Forum Uranium Corporation did not cover the entire area of interest, this data set was required to fill gaps.

LANDSAT-7 data available online at http://www.geobase.com were used in conjunction with digital terrain models (DTM) of the area of interest. Coupled together, the imagery and elevation data provide valuable information on surficial geology, overburden material, and structural trends because these features commonly have diagnostic topographic responses. To accentuate the outcrop distribution of a prominent quartzite unit it was found that a false colour RGB image based on bands (RGB = 745) emphasized these features.

METHODS

Source-edge detection (SED) routines (Fig. 3a, b, c) were run on multiple apparent resistivity grids (140 kHz, 40 kHz) and magnetic grids using Geosoft's Source Edge Detection GX (Blakely and Simpson, 1986). Higher frequency EM data were used as they tend to outline geological features at shallower depths in particular areas with thin overburden or outcropping bedrock. Edges within grids were primarily defined through use of the horizontal gradient operator. For magnetic data analytic signal and pseudogravity transform procedures were also used to double check solutions as suggested by Pilkington and Keating (2004).

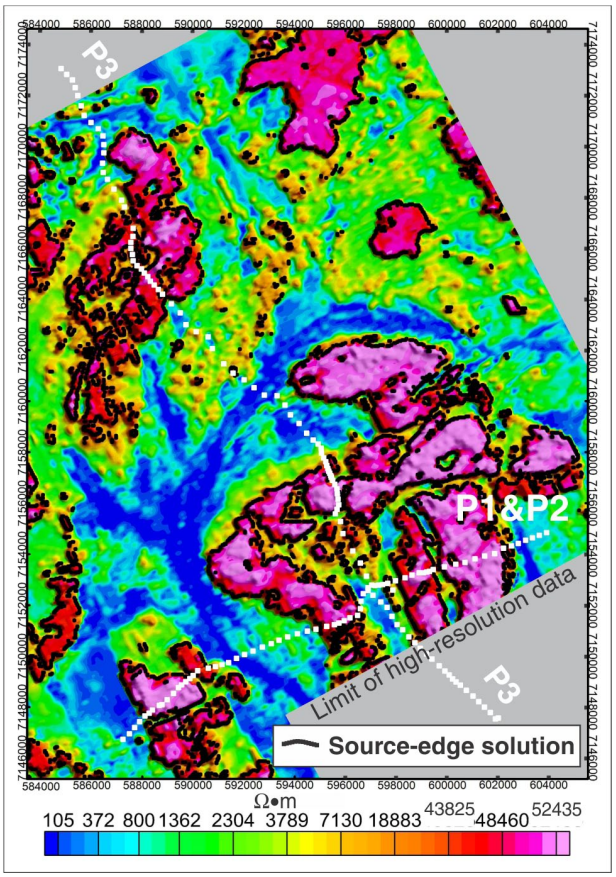

Figure 3. a) Source-edge detection (SED) results for 140 kHz resistivity grid. Labels "P1&P2", and "P3" for gravity stations from Figure 2 (white squares) are provided for spatial context only.

For the high-resolution magnetic data only solutions with a value more than 0.5 nT were kept. The relatively high cutoff limited the total number of solutions which improved processing time and selectively removed those which are indistinct. Source-edge detection was also performed on the coarser regional magnetic data, but the limited resolution restricted its ability to provide any new insights not observed in the higher resolution grid. Electromagnetic grids were processed similarly with a minimum cutoff of 50 Ω•m and 90 Ω•m for the 140 kHz and 40 kHz resistivity grids, respectively.

Having adequate geological constraints is critical to the success of any geophysical model exercise. The existing geological mapping summarized by Hadlari et al. (2004) provided the original klippe concept for testing and the broad lithostructural framework for the design of models in this study. An extract from that mapping for the study area is reproduced without any changes in Figure 4a, except that certain structural features recognized by that mapping are labelled for comparison with products of this study.

Rock physical property data (Table 1) were assembled to provide constraints on modelling solutions from the geophysical observations. Specific gravity and magnetic susceptibility

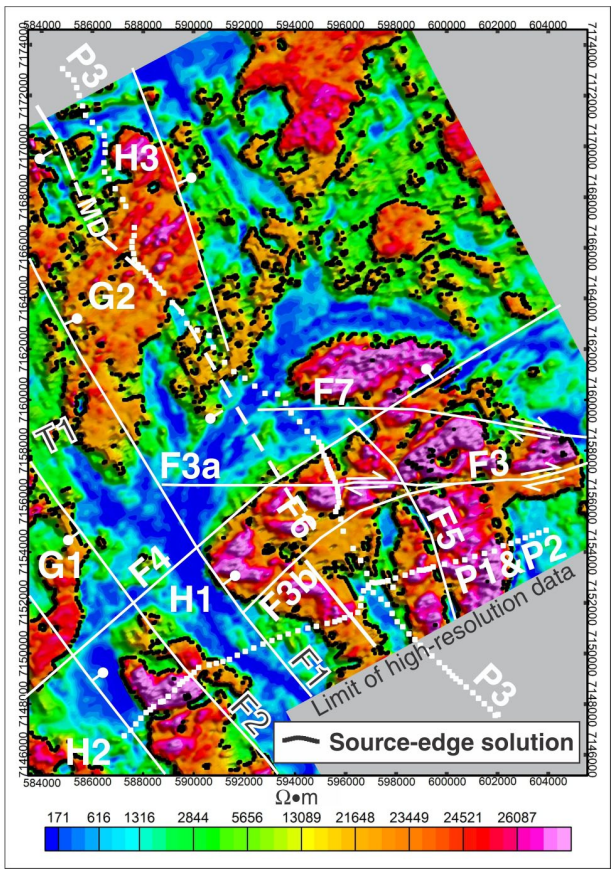

Figure 3. b) Source-edge detection results for 40 kHz resistivity grid. Labels F1 through F7 refer to interpreted faults; all discussed in text. Faults are from Figure 1, advanced from previous fault knowledge reproduced in Figure 4. Labels "P1&P2", and "P3" for gravity stations from Figure 2 (white squares) are provided for spatial context only.

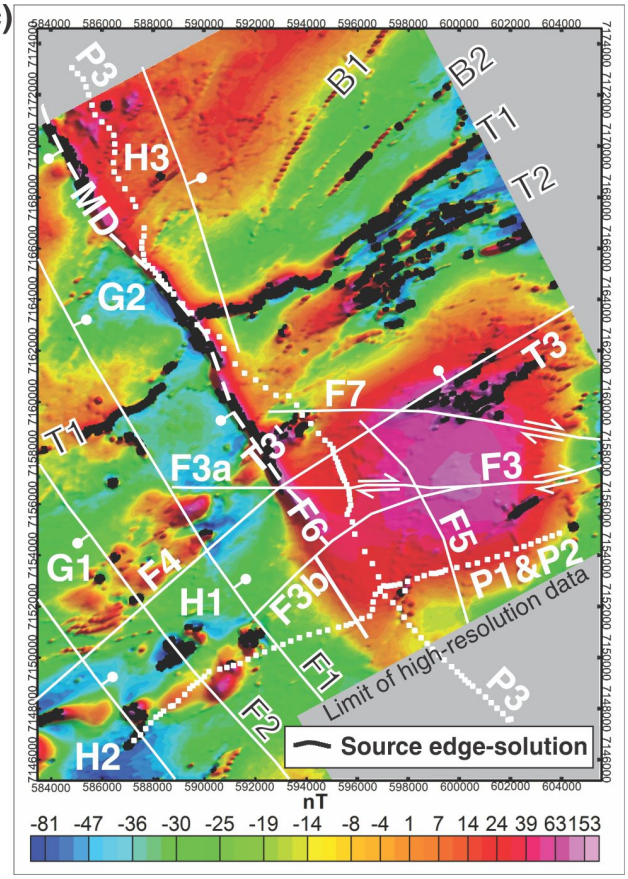

Figure 3. c) Source-edge detection results for total-aeromagnetic intensity map. Labels F1 through F7 refer to interpreted faults; B1, B2, T1, T2, and T3 refer to interpreted dykes that are only expressed in the aeromagnetic data; all discussed in text. Faults in Fig. 3c) are from Figure 1, advanced from previous fault knowledge reproduced in Figure 4. Labels "P1&P2", and "P3" for gravity stations from Figure 2 (white squares) are provided for spatial context only.

of 13 samples from the klippe area were measured and averaged. These samples represent only the Ketyet River group, therefore density and susceptibility values by Thomas and Wood (2007), Hasegawa et al. (1990), Tschirhart (2009), and Tschirhart et al. (2011b) were included to represent the remaining units in the study area.

Source-edge detection solutions were imported into ArcGIS to create a new map that predicts the distribution of a number of geophysically distinctive units using only the source-edge solutions (Fig. 4b). This new map is closely related to topography because most of the topography is controlled by the resistance to erosion of the quartzite relative to other rock types.

Unconstrained three-dimensional (3-D) magnetic inversions were run using the UBC-GIF Mag3d code (Fig. 5a, b, c, d, e). A 3-D mesh file defining the bounds of the inversion data was created using Encom Modellvision™. Synthetic north-south flight lines spaced 160 m apart were created over the high-resolution magnetic data set with data points being sampled at 160 m intervals along each line. A mesh file containing voxel cubes set to 240 m x 240 m x 25 m was then exported to UBC-GUI. The model was limited to a depth extent of 10 km, which had to be used because the broad regional anomaly at depth would limit the ability of the program to resolve any fine details. A depth increment factor of 1.1 was used which consecutively multiples every cell in the Z direction below the top cell by 1.1. In this configuration, the top cell had a depth extent of 25 m while the deepest voxel cell had a depth extent of 1029 m.

Of critical importance to the inversion model is how noise within the data is treated. Noise limits the amplitude of the anomalies that will be solved in an inversion, and can be reduced by nulling large values, reducing the total dynamic range (Williams, 2008). A noise level of 5% was used in the inversion. The inversion was run using the generalized crossvalidation (GCV) mode producing a computer calculated tradeoff parameter, which implements crossvalidation analysis on the inversion without positivity (Spicer, 2010).

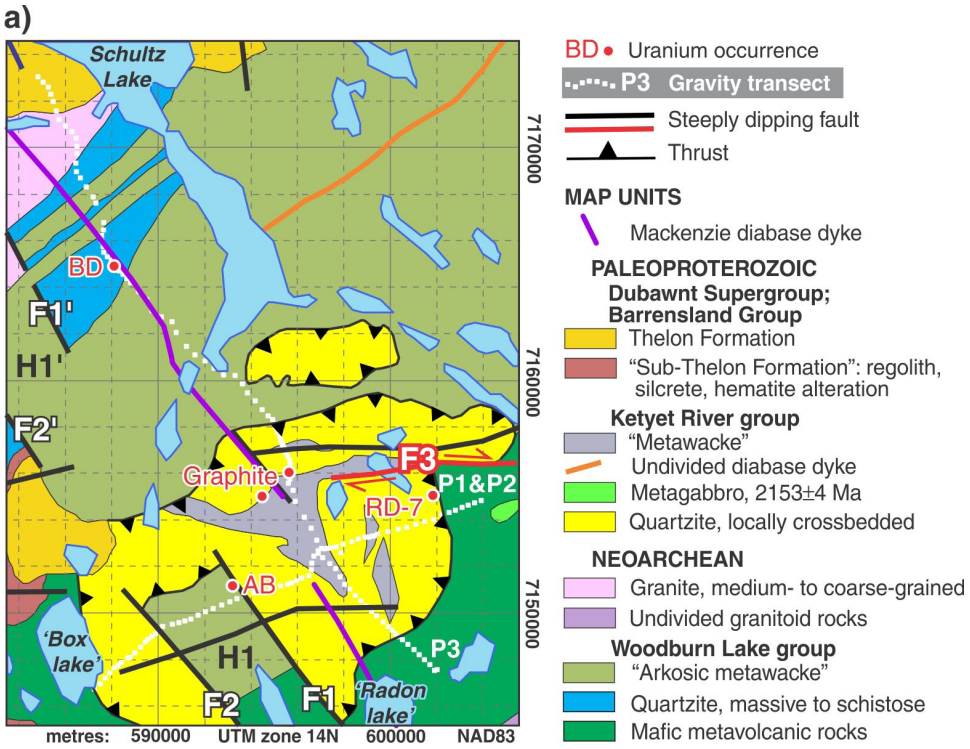

Figure 4. a) Original geology of the study area from Hadlari et al. (2004). The labelled faults F1 through F3 and horsts (H1, H1') roughly correspond to the current interpretations on Figure 1 that are transcribed to Figure 3c and later figures, and discussed in text. The legend comprises only those units that Hadlari et al. (2004) mapped within the study area, using definitions simplified after Hadlari et al. (2004), but with the new colour scheme of Figure 1 to facilitate comparison. 'Metawacke' of the Ketyet River group is now termed 'grey schist' and the Neoarchean quartzite is now assigned to Ketyet River group quartzite throughout this paper.

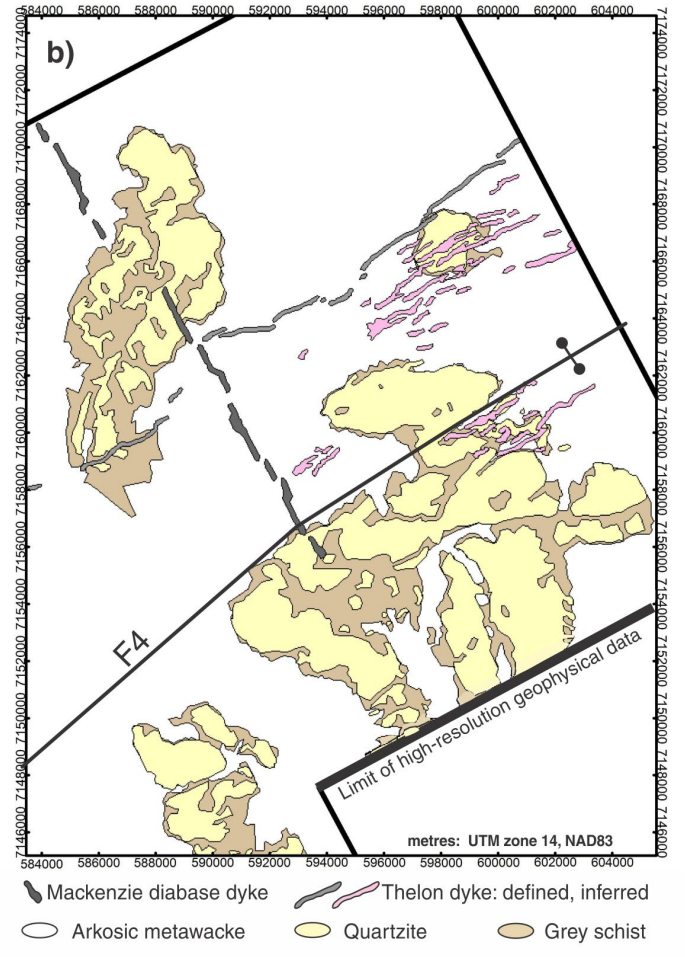

Figure 4. b) Predicted distribution of five major bedrock units in the same study area, interpreted entirely from source-edge detection solutions for electromagnetic and aeromagnetic data (Fig. 3). 'Thelon dyke' comprises two components both trending 075°: a swarm of small dykes outlined in pink, interpreted entirely from aeromagnetic data, and a large, single dyke in medium grey that corresponds to the "undivided diabase dyke" of Figure 4a. The F_4 denotes a steeply dipping, dextral and/or normal fault that was newly interpreted here from combined lineament analysis of aeromagnetic, electromagnetic, and gravity data.

The alpha versus length scales define the model objective function, or more simply the balance of smoothness versus smallness in the model (Williams, 2008; Spicer, 2010). These values were defined by length scale in each of the three directions Le, Ln, Lz as 960 m, 960 m, and 960 m, respectively.

Three forward-model profiles (P1, P2, P3) of the study area (Fig. 6) were created using Geosoft's GM-SYS GX along the orthogonal gravity transects shown in Figure 2. The rock properties (Table 1), source-edge detection solutions on electromagnetic and aeromagnetic data (Fig. 3, 4b), preliminary geology (Fig. 4a), and the unconstrained 3-D magnetic inversions were integrated to infer the 3-D locations of lithological units to which uniform physical properties had been assigned. Classified LANDSAT-7 imagery and digital terrain models were visually inspected to further constrain the quartzite boundary based on the distribution of outcrops, based on the principle that the quartzite is present only where it outcrops. After near-surface boundary conditions were set as above, deep modelling relied primarily on free-air gravity data because the supracrustal assemblages have insufficiently magnetic contrasts for modelling aeromagnetic data, and the EM data reflect mainly shallow elements. The only unit strongly influenced at depth by the aeromagnetic inversion is the granitoid pluton that is not exposed in the study area.

RESULTS AND DISCUSSION

Because this study was developed and completed in parallel with a detailed mapping study the results of which became available mainly after modelling was completed, this study had to rely mostly on pre-existing data (Hadlari et al., 2004) and very preliminary results of the mapping by McEwan (2012). Similarly, the latter could only incorporate preliminary results of this study before developing their synthesis and conclusions; however, this study and that of McEwan (2012) were both used as sources of knowledge for the regional synthesis that in turn contributed Figure 1

Table 1. Rock properties used for modelling. NA = not applicable.

Rock type	Number of samples	Density range (g/cm^3)	Mean density (g/cm^3)	Magnetic susceptibility range (x 10^{-3} SI)	Mean susceptibility (x 10^{-3} SI)
Quaternary sediment (overburden[1])	Unknown	1.5–2.00	2.00	Unknown	Unknown
Mackenzie dyke[2]	1	NA	2.73	NA	20
Thelon Formation	26	2.21–2.85	2.56	0–1.0	0.3
Ketyet River group					
Quartzite	8	2.62–2.68	2.66	0–0.027	0.01
Grey schist	5	2.63–2.71	2.68	0–0.11	0.05
Granitic rocks					
Snow Island granite to gabbro (dated[3] as 2.6 Ga in the north)	1	NA	2.72	Unknown	Unknown
Snow Island or Hudson granite (inferred at depth)[2]	1	NA	2.56	NA	1.8
Woodburn Lake group					
Banded iron-formation[4]	3	2.98–3.39	3.18	0–11.3	11.3
Arkosic metawacke[1] (Pipedream assemblage)	1	NA	2.71	Unknown	Unknown
Metasediments[2] (Pipedream assemblage)	29	2.31–2.84	2.64 (not used)	0–77	3.9
Metavolcanic rock-dominated supracrustal gneiss[2] (Halfway Hills assemblage)	6	Not reported	2.70 (used 2.61 in the north)	Not reported	12.4

[1]Hasegawa et al. (1990)
[2]Tschirhart (2009)
[3]Hadlari et al. (2004)
[4]Thomas and Wood (2007)

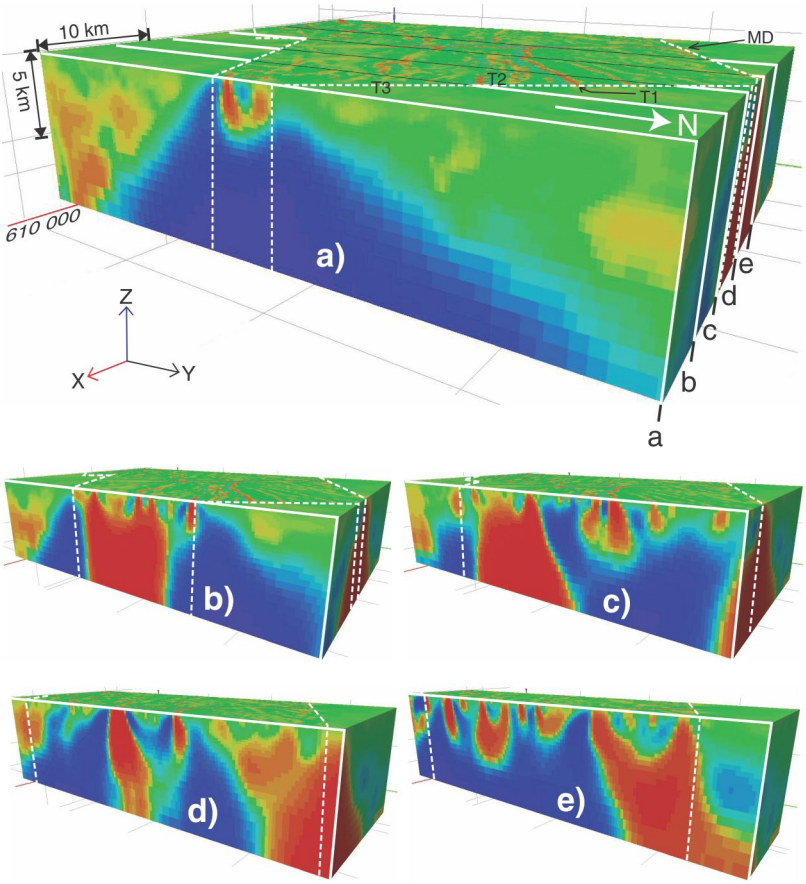

Figure 5. Unconstrained inversion of aeromagnetic data looking southwest. Dashed white lines outline the limits of the high-resolution data. Outside of these boundaries, generalized data are included to reduce model edge effects, but have little geological significance. **a)** Entire block; top surface represents 2-D aeromagnetic data as in Figure 3c, but with different dynamic range; MD, T1, T2, and T3 indicate dyke sets: Mackenzie, defined Thelon, and two sets of inferred Thelon (as in Fig. 3c). Planes of block cross-sections are outlined by solid white and fine black lines labelled 'a' through 'e'. **b)** A 5 km slice removed from east side of block. **c)** Ten kilometres removed from east side of block. **d)** Fifteen kilometres removed from east side of block. e) Twenty kilometres removed from east side of block. *See* text for discussion.

back to this study. Some issues and discoveries are discussed below, including how they affect confidence in the resulting geological models produced by this study.

Mapping geological contacts

When this study began the most recent published geological map for the Forum Uranium Corporation project area was at 1:250 000 scale (Hadlari et al., 2004) and is the source of Figure 4a. As noted above, the geology of Figure 4a does not match that part of Figure 1 because Figure 4a represents the original geology map when this study started, whereas Figure 1 represents the new geology map that began with Hadlari et al. (2004) as a base, and was influenced by the results of the GEM Uranium Project compilation and new detailed geoscience research, including this study. The 2004 map comprises three main surface rock units in the core part of the study area: arkosic metawacke of the Pipedream assemblage, Woodburn Lake group, and quartzite and metawacke (now termed grey schist in Fig. 1) of the Ketyet River group. The southern part of the map area was mapped by Hadlari et al. (2004) as predominantly mafic metavolcanic rock of the Woodburn Lake group, here assigned to the Halfway Hills assemblage. Hadlari et al. (2004) also interpreted a major structural discontinuity between a klippe of Paleoproterozoic quartzite and grey schist, and the structurally underlying Pipedream and Halfway Hills assemblages of the Woodburn Lake group. The klippe hypothesis framed questions for this study to answer and thereby guided placement of the gravity transects. Are the quartzite and grey schist a discrete Paleoproterozoic package separated from the Woodburn Lake group by a klippe, or are these units structurally intercalated, or is there a combination of these structural relationships? How deep does the quartzite extend beneath the study area?

For optimum testing of these geological questions, as well as to test the depth and nature of an unexposed and presumably deep granitic pluton inferred from the large aeromagnetic high beneath the klippe, the available map required refinement so that it correlates more closely with topographic, geophysical, and LANDSAT data (Fig. 2). In particular the authors needed to test and refine the apparent correlation between quartzite and topographic highs that was observed during 2010 fieldwork. Therefore, the first step of this study generated a more detailed remote predictive lithological map of the area based on the available aeromagnetic, LANDSAT-7, and EM data sets (Fig. 4b). This provides a more precise distribution of quartzite versus grey schist versus Pipedream metawacke at and near the surface within and around the klippe area, and reinforces the general observation that where quartzite is present there is a hill with outcrop, and where grey schist is present there is a slope or valley with sparse outcrop. The synthesis of these

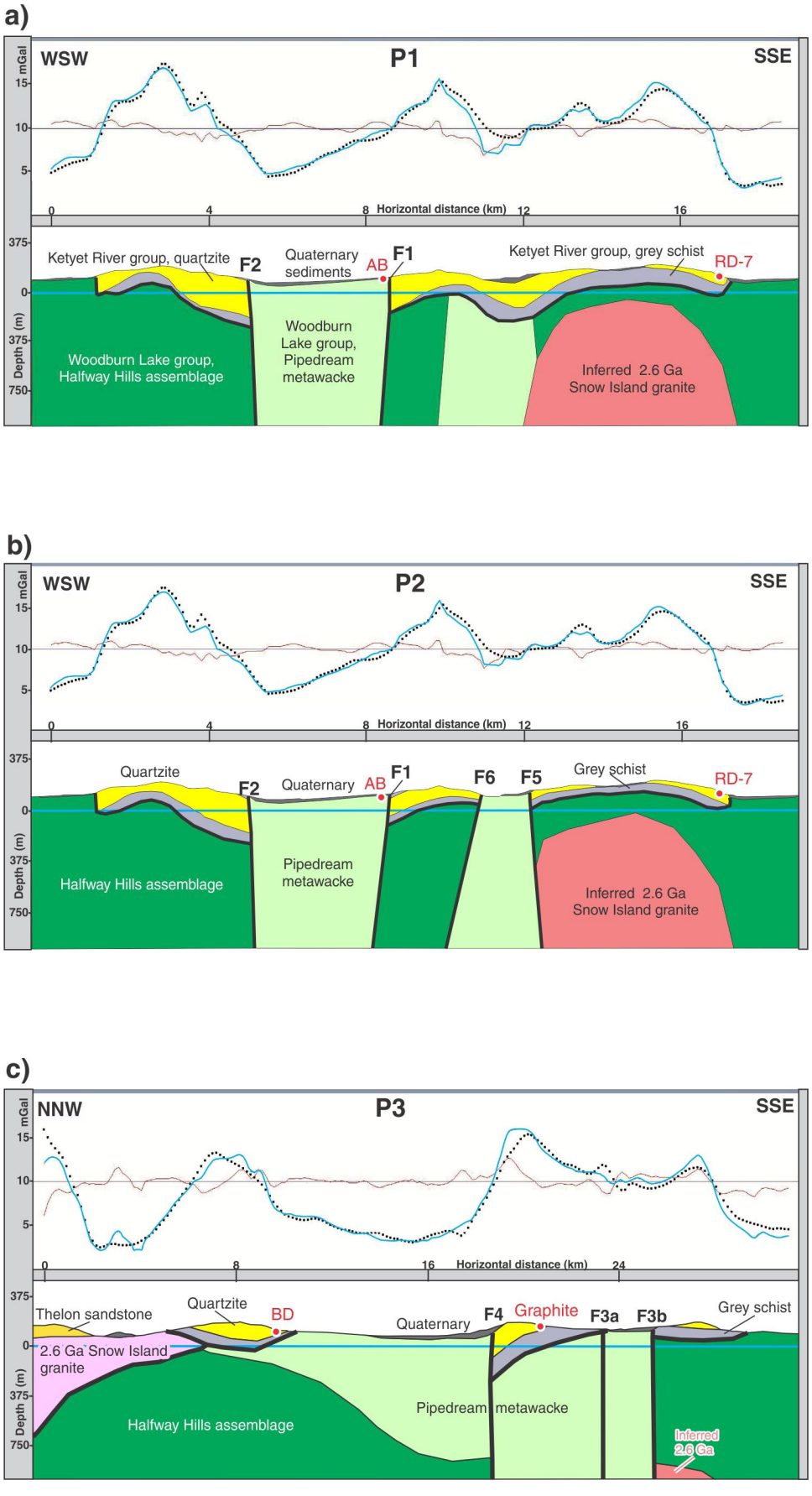

Figure 6. a), b), c) Forward-model profiles P1, P2, and P3 oriented along the gravity transects shown in Figure 2. In the top panel of each profile: dotted line = observed gravity, blue line = modelled gravity, and red line = deviation of modelled gravity from observed gravity. In the bottom panel of each profile, inferred major subhorizontal structural discontinuities (heavy lines) roughly correspond to thrust faults shown in Figures 1 and 4a. Inferred steep faults (heavy lines) are labelled as to their possible counterparts in Figures 3 and 4 and following. Uranium occurrences are shown in red.

diverse data sets proved to be very successful as each data set covered off limitations in the other sets to define most of the quartzite–grey schist contacts. Parallel fieldwork by B. McEwan (2012) and Jefferson et al. (in press) reconfirmed the predictive value of the geophysical guidance in several places, and in turn is part of the process of further refining the regional geological map the current version of which is in Figure 1.

The surface units of quartzite, grey schist, and Pipedream metawacke have little magnetic contrast, however, the quartzite is distinctly more resistive than the grey schist, and the arkosic metawacke is intermediate in resistivity. The EM and topographic information is thus crucial for defining surficial contacts, most importantly the discontinuity separating the quartzite and grey schist from the underlying Pipedream metawacke (Fig. 4b, 6, 7, 8). The use of different EM frequencies allowed for the determination of lithological changes with increasing, but still shallow depth. The high-frequency grid (res140k) defines very near-surface contacts and the lower frequency grid (res40k) reveals slightly deeper contacts. The depth penetration is limited to the few upper tens of metres due the restricted depth penetration of EM and, in the valleys, by conductive surficial deposits and water bodies.

Source-edge solutions on the magnetic data failed to define geological contacts of near-surface units because none of the three (quartzite, grey schist, arkosic wacke) contain magnetite. Magnetic data do, however, define a major, but discontinuous 170° dyke interpreted as belonging to the Mackenzie dyke swarm that transects the middle of the study area, and a swarm of the 070–080° Thelon dykes that transect and lie north of the klippe (Fig. 1, 3c, 5c).

A number of folds and faults previously unidentified in the basement complex are suggested by the SED analysis. Two northwest-trending fold noses are inferred in a selected central portion of the TMI map, just south of the fault labelled F5 in Figure 7. Future testing of such structures could be accomplished by applying a cutoff level to incorporate them into the SED solutions, and by reanalyzing detailed structural data collected by McEwan (2012) in this locality. McEwan (2012) also mapped tight, enigmatic, northwest-trending folds north of the Graphite occurrences. Possibly such folds are local effects of or add to the geophysical expression of the F5 fault.

Offsets of electromagnetic and aeromagnetic linear features parallel to and crosscutting the 150° Mackenzie dykes and 075° Thelon dykes may also contribute to knowledge regarding faulting in the area. The dykes constrain the timing of faulting and deformation, depending on their orientations, although it is not certain without detailed study whether the dykes occupied pre-existing faults or were intruded during faulting. In any case, most of the dykes postdate ductile D_1 and D_2 folds in the metasedimentary rocks, although some bostonite dykes are parallel to F_2 axial planes.

New knowledge and ideas for further testing have been added to the map database in a number of places. Pipedream metawacke is predicted by the SED routine to form basement inliers within the centre of the structure. This prediction was verified by 2010 and 2011 field traverse data. The quartzite–grey schist package in the southwest corner of the study area was previously mapped as continuous from 'Box lake' (informal name), around the north end of the H_1 horst, and on down almost to 'Radon lake' (informal name) (Fig. 4a); however, analysis of resistivity in this study indicates that they are separated, likely as a result of erosion after development of the H1–H1' horst. In 2011 fieldwork by the third author confirmed that the Pipedream assemblage does separate the two areas of quartzite. One discrepancy that requires further analysis is the style of deformation in the northwestern part of the map around Forum Uranium Corporation's BD showing. The existing maps (Fig. 4a) as well as new mapping by Jefferson et al. (in press) (northeastern Fig. 1) show this as a complex zone of tight, upright, second-generation folds involving both Woodburn Lake and Ketyet River groups. In contrast, the SED

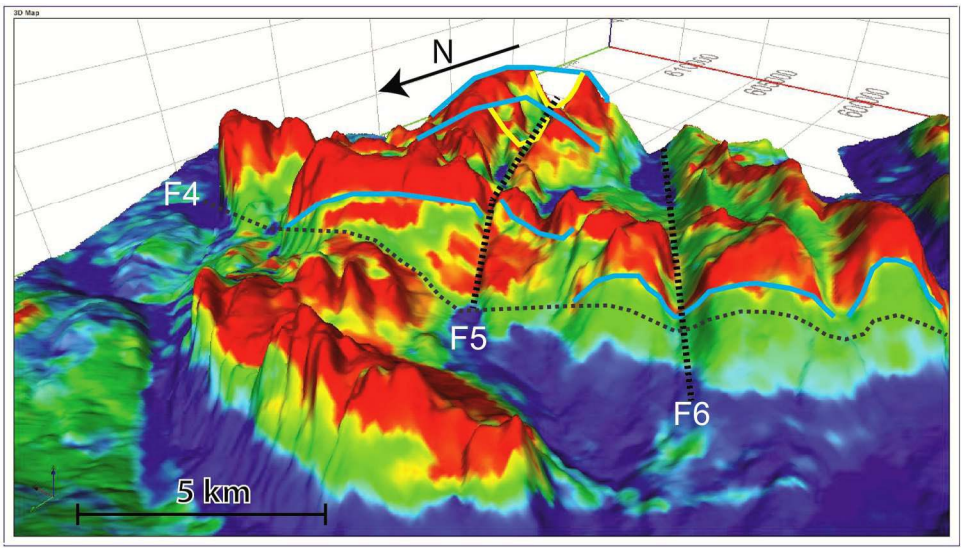

Figure 7. Resistivity at 140 kHz draped on topography with 20x vertical exaggeration. Outlined in light blue at top centre is the proposed single large antiform. Yellow lines outline alternative hypothesis of antiform-synform-antiform. The enveloping surface of the fold (black rectangle) appears to dip toward the east. Selected predicted near-vertical faults F4, F5, and F6 are shown by dotted lines. Other apparent folds (blue lines on west side of structure) are discussed in text.

(Fig. 4b) suggests a simpler thrust sheet of the Ketyet River group overlying the Woodburn Lake group rocks. Because the folds and steep dips are well defined at surface, the SED interpretation suggests that the surface complex is separated from a deeper structural panel by a gently dipping detachment modelled in this paper. In the revised regional map this SED solution is incorporated by showing the upright fold complex as forming the upper plate of a larger detachment.

Interpretations of the data suggest that much of the central klippe detachment surface is offset by steeply dipping brittle faults (Fig. 1, 3, 4, 6, 7, 8). Significant faults suggested by the aeromagnetic data (F1 through F5 of Fig. 3c and 4a) are supported by lineament analysis of electromagnetic (Fig. 4b) and topographic data, and most likely postdate development of the thrust surface. North-northwest-trending faults along the west side of the map area (F1 and F2 of Fig. 3c) appear to displace the quartzite approximately 15 km in a sinistral sense, but this offset is most likely a result of differential erosion across a horst (H1, H1' of Fig. 4a) that is bounded by those faults. A set of east-northeast-trending faults also displaces the northern third of the klippe some 5 km dextrally (F3, Fig. 3a). These dextral faults are consistent in style with the Thelon, Judge Sissons, Gerhard, and additional minor 075° faults in the Kiggavik deposits area.

Inversion modelling

A broad lithological result of the unconstrained aeromagnetic inversion is to outline the domal top of a deep-seated pluton with a mafic component. This dominant, relatively broad, deep-seated, highly susceptible magnetic anomaly is a challenge to invert because only conceptual geological

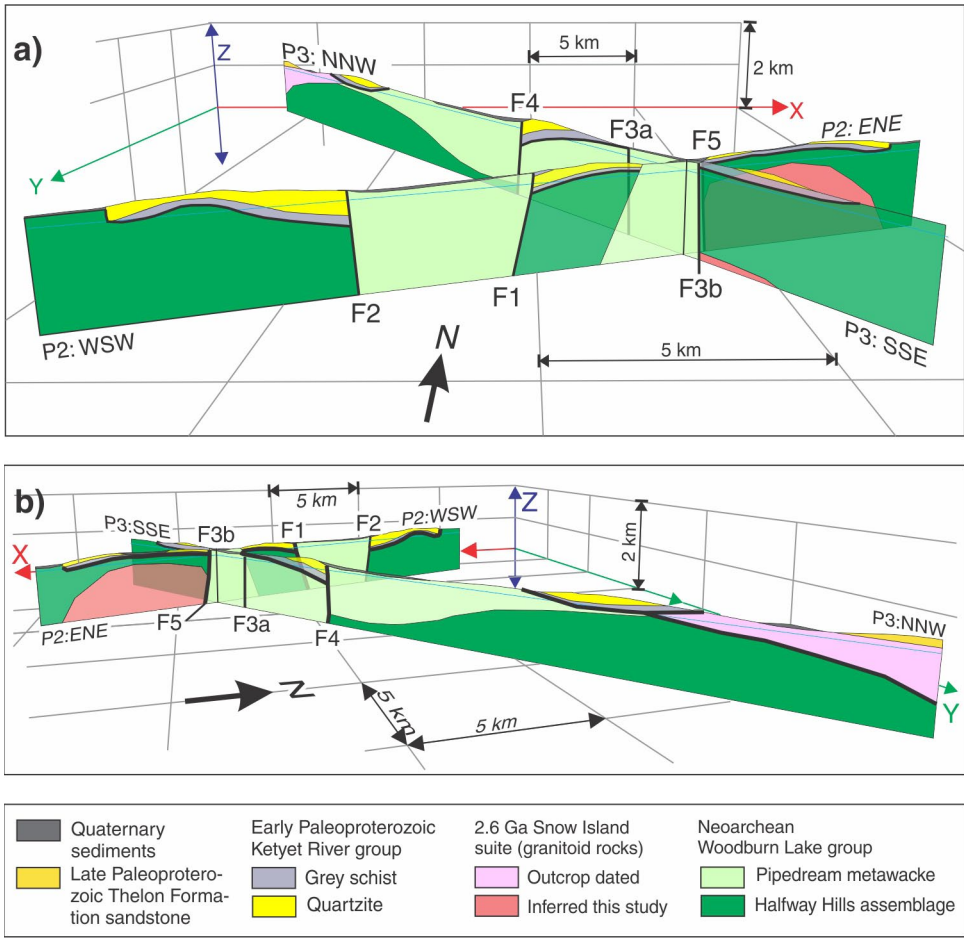

Figure 8. Cross-sections P2 and P3 from Figure 6 shown in perspective with each other; vertical exaggeration 5x. **a)** Looking toward 000°. **b)** Looking toward 200°. Heavy black lines denote major structural discontinuities, both steeply and shallowly dipping as discussed in text. F_1, F_2, and F_4 correspond to faults mapped in Figures 1, 3c, 4a, and 4b. Caveat: as discussed in text, these models are not intended to be fully geologically balanced at this stage, but do indicate one possible set of configurations that account for the observed geophysical signals and may be considered in developing balanced geological cross-sections.

and geophysical constraints can be used. The unconstrained inversion modelled the geometry as a steep-sided, deep plug. Although geologically reasonable, this solution may be the result of the unconstrained inversion process. Furthermore the relationship between surface geology and this plus other broad anomalies is inconsistent, as follows.

The interpreted deep-magnetic anomaly underlying the centre of the study area is northwest of a much larger and more intense aeromagnetic anomaly of otherwise similar style, south and east of Judge Sissons Lake (Fig. 1). In that area, a granitoid batholith with abundant marginal xenoliths has yielded a U-Pb zircon age of 2606 +4/-3 Ma (unpub. data by Roddick and LeCheminant, reported by Hadlari et al. (2004)). Granite in the northwest corner of the study area (Fig. 4a) has been dated as about the same Neoarchean age (2608 +28/-10 Ma; unpub. data by Roddick and LeCheminant, reported by Hadlari et al. (2004)), but has no significant underlying gravity or magnetic anomaly. The ca. 1830 Ma Hudson granite–Martell syenite suite (Peterson et al., 2010) generally has high magnetic susceptibility (P.A. Tschirhart, unpub. data, 2009); however, the Hudson suite is characterized as being tabular to sheet-like intrusions (Scott et al., 2010; Tschirhart et al., in press) with laterally extensive magnetic anomalies that have sharp edges such as west of Kiggavik. The magnetic inversion (Fig. 5) solved the pluton as a vertical-walled cylinder (inconsistent with the Hudson suite), and it coincides with a gravity low. The Nueltin granite suite has steep-walled plutons; however the northernmost mapped large Nueltin granite is at Mallery Lake, some 90 km southwest of the study area, and is an aeromagnetic low (T. Peterson, unpub. data, 2012). Other Nueltin granite bodies spatially associated with the Kiggavik camp deposits are very small. The best candidate for the deep pluton is the late Neoarchean Snow Island suite (Peterson and Born, 1994). Similar coincident gravity lows with magnetic highs are associated with two 2.6 Ga granite bodies mapped by Hadlari et al. (2004) in the northwest corner of the study area and immediately south of the study area.

Solutions from the unconstrained inversions for upper crustal structures have generated only straight linear features. Most lithological units in the Woodburn Lake and Ketyet River groups are nonmagnetic. Banded iron-formation units with very high magnetic susceptibility are known elsewhere within the Tehek-Marjorie belt, but appear to be absent from the study area. Thus, there are no magnetic marker units that might define ductile deformation structures.

The linear features evident in both the raw total-magnetic-intensity data (Fig. 3c) and the inversions (Fig. 5) are useful for mapping faults and dykes that are possibly related to development of the Thelon Basin. For example, a set of gently arcuate, subtle to distinct (B1, B2) magnetic linear features trending 015° to 045° is evident northwest of the main Thelon dyke (T1 in Fig. 3c). These correspond to poorly exposed bostonite (fine-grained highly potassic syenite) dykes, two of which (B1, B2) were field verified in 2011. Such dykes typically are poorly exposed, but are evident as lines of syenite boulders that generate 200 to 300 counts per second with elevated K, U, and Th on field spectrometers. The fine-grained mafic syenite dykes are interpreted as derived by a mixing of lamprophyre with Hudson granite (Peterson et al., 2010) and have three orientations in the region of Figure 1: 015–050°, 080–100°, and 165–180°.

Two sets of repeated linear magnetic highs labelled T2 and T3 in Figure 3c are parallel to the major Thelon dyke (T1), which regionally (Fig. 1) has orientations between 060° and 080°. Interpretation of these arrays of thin aeromagnetic linear features as being part of the Thelon dyke swarm is based on the parallel, straight, multiple, segmented, linear nature of these anomalies, and their limited local amplitudes that are considerably less than those of banded iron-formation units in the region, but within an order of magnitude of that of the major Thelon dyke (T1). The linear anomalies might represent iron-formation beds that are thin enough to have only moderately high magnetic susceptibility, however iron-formation is unlikely to form multiple parallel sets with such short strike lengths. Iron-formation units typically form single, elongate, continuous folded markers and, in the vicinity of Judge Sissons Lake, have far higher magnetic susceptibilities than dykes. A third possibility for the clusters of magnetic linear markers is lamprophyre or bostonite dykes like B1 and B2 discussed above. In any case, the interpreted small Thelon dykes provide information on the late brittle extensional structural and right-lateral strike-slip stress regime that was in existence during their intrusion: approximately 1830 Ma if part of the Hudson suite; 1750 Ma if part of the Nueltin Suite.

A set of 100° to 110° dextral faults (F3 in Fig. 3c) transects the broad aeromagnetic high, abruptly terminating the southwest end of one swarm of Thelon dykes (T3). These faults were recognized by Hadlari et al. (2004) as represented in Figure 4a, were more precisely mapped by McEwan (2012), and are further refined and incorporated into the regional map (Fig. 1) based on this study. The main F3 strike slip fault clearly offsets the quartzite dextrally and has a strong linear expression in the resistivity data. The northern strike-slip fault (F7) appears to offset the T3 swarm some 6 km dextrally from its inferred continuation at T3'; however, the dextral faults do not appear to affect the major Thelon dyke (T1).

Major dip-slip faults were previously mapped parallel to the 155° Mackenzie dyke swarm by Hadlari et al. (2004) (Fig. 4a). As shown in Figure 3c a Mackenzie dyke (MD) is parallel to, but does not occupy the mapped faults, and neither the dyke nor the normal faults appear to significantly offset the magnetic expression of the major Thelon dyke (T1) geometrically, although this dyke and the T2-T3 dyke swarms have a diminished magnetic expression in the graben (G1, G2). The previously mapped northwest-trending dip-slip faults are clearly evident as linear features on the LANDSAT-7 image and have major offsets that resulted in a central horst (H1, consistent with the discussion of resistivity data, below). Given that the southeast side of

the Mackenzie dyke lineament has a much lower magnetic expression than the northeast side; it is interpreted as having a previously unrecognized dip-slip offset: southwest side down. Curiously, a dip-slip fault is not consistent with surface geology where the dyke ends to the south, as there is no LANDSAT lineament and no offset of the well exposed quartzite. A second graben (G2) newly recognized here, flanked in part by the Mackenzie dyke, is separated by a horst (H1) from the earlier recognized graben (G1) that in turn is flanked by a second horst (H2) to the west (Fig. 3c).

In summary, many geological entities have aeromagnetic expressions. With respect to the inferred large pluton, as shown by Spicer (2010) in a simple geometric model, unconstrained inversions have limited success at defining the lateral morphology of a source body. Though the tops may be well defined, the sides, unless constraints are applied, will be modelled as near-vertical walls continuous to depth. The deep plutons are intriguing features and warrant further analysis on a regional basis. It is thus concluded that for many geological problems inversion models are very useful, but in areas where nonmagnetic units are the topic of interest, other geophysical methods are required.

Forward modelling: west-southwest profile

Two different models P1 and P2 (Fig. 6a, b) were created along the east-northeast–west-southwest detailed gravity transect (Fig. 2), and one model was created along the north-northwest–south-southeast transect (P3) in order to interpret the structure of the area. Bodies were modelled as 2.75D, i.e. the source body must have an arbitrary constant cross-section of finite length that is perpendicular to the observation profile. The free-air gravity anomaly across the P1 and P2 profiles has a maximum dynamic range of approximately 10 mGal. Interpretation of this observed range must take into consideration elevation differences across the profile in order to decide how much of the anomaly is assignable to the underlying geology. At first approximation, the gravity anomaly is related to elevation and the presence of quartzite, but is independent of the aeromagnetic variations, based on the following examples. A gravity low 2 km from the eastern end of the P1 and P2 transect is coincident with a magnetic high. Southwest along this profile a dense unit is required to account for the gravity peak that begins in a valley, but stays high across the first ridge to the west. On the southwestern side of the P1 and P2 transect the gravity signal again rises in a broad valley.

The starting model P1 (Fig. 6a) is based on the geological interpretation of a thin structural panel comprising overturned Paleoproterozoic quartzite structurally underlain by grey schist, separated by a laterally extensive discontinuity from underlying Pipedream metawacke; however, several key changes had to be made to the geological model in order better approximate the observed gravity signal. First, the wavelength of the antiform-synform-antiform configuration on the eastern side of the structure was changed to a single large antiform based on 3-D analysis of the electromagnetic signal and relationship to topography. Near-surface contacts obtained by edge detection of EM data were draped on topography that was vertically exaggerated to enhance any topographic expression of the geological structure (Fig. 7). The shape of the contact draped over topography appears as a single large fold rather than multiple small folds. Smaller folds are suggested by the data on the east side of the klippe, but converge into a single fold where the profile intercepts them. These folds are relatively open — they could be second generation as defined by McEwan (2012), or even later structures.

Second, new steeply dipping faults were introduced (F5, F6) and a significant change was modelled across F_3 which has two possible western extensions 3a and 3b where it crosses the P3 transect (Fig. 3b, c). With respect to the above-discussed folds inferred from the electromagnetic data, a conductive valley along the axis of the most easterly inferred antiform appears to be the result of a fault (F5 in Fig. 7). In this case, the fault acted as a line of preferential erosion that exposed the structurally underlying schist, thereby producing the same response as would an antiform-synform-antiform in the EM data. It is also unlikely that the quartzite would change its relative position to underlie the schist over such a small distance because the quartzite resists erosion, following the general rule that where there is quartzite it outcrops. The second change to the previous geological interpretation is the introduction of a dense Pipedream metawacke body below the thrust surface. This proposed hidden unit is required to account for the gravity data, and there is no other surface explanation available.

The southwest side of the 2004 geological map (Fig. 4a) invokes a fault-bounded horst (H1) with Pipedream metawacke in the middle and Paleoproterozoic quartzite on each side. Within that horst, the 2004 mapped geological contact between Halfway Hills assemblage mafic metavolcanic rocks on the south and Pipedream arkosic metawacke on the north is located some 8 km southeast of where it is mapped outside of the klippe to the east and west. Thus, one or more of the previously mapped contacts are in error, or the contact dips gently south so that erosion of the horst moved this contact south, or the fault block was extruded toward the southeast between opposing strike-slip faults. In all three possibilities, subvertical faults are required to suit the gravity signature. Since this geophysical analysis was conducted, further mapping has modified the mapped contact between Pipedream metawacke and Halfway Hills mafic metavolcanic rocks, taking into account these geophysical constraints (Fig. 1). For example H1 is continuous with H1', F1 and F2 are continuous with F1' and F2' respectively, and the Pipedream metawacke outcrops much farther southeast on the east side of the horst — the metagabbro shown on Figure 4a is a sheet hosted by Pipedream metawacke.

Profile P2 is based on the same data as P1, but differs in two ways. The first difference is that the anomalously dense basement Pipedream metawacke on the east-northeast

side of the profile in P1 was continued up to surface and the overlying Ketyet River group rocks were removed. This better conforms to the gravity data, but also satisfies the edge-detection routine that suggests there may be some basement exposed at surface in the middle of the structure, just south of the Graphite showings. Subsequent outcrop mapping confirmed the presence of Pipedream metawacke as predicted. The sides of this basement block are bounded by near-vertical faults resembling a horst. If this in fact is a horst structure it could account for why the quartzite in this region has been locally eroded, but is still present at the flanks. The proposed faults are coincident with topographic lineaments visible on LANDSAT-7 and have been incorporated in revisions to the regional geological map by the third author. The second major differences are in the amplitudes and wavelengths of the folds near the east-northeast end of the model profile. Lower amplitude, longer wavelength folds in the Ketyet River group better fit the gravity data and seem to be more topographically accurate.

A low-density pluton with a vertical cylindrical shape was introduced to the gravity model in conformance with the magnetic inversion model (Fig. 5a, b, c). The density value, $\rho = 2.54$ g/cm^3, is close to that recorded from field measurement, $\rho = 2.56$ g/cm^3, for both Nueltin and Hudson granite. This low density was chosen rather than continuing the anomaly closer to surface because the result is more compatible with that of the magnetic inversion, and because there is no known contact metamorphic effect of an intrusion. This pluton complicates the model because it locally drives the gravity signature, yet results from the magnetic inversion suggest that the top of the pluton is too deep to incorporate into the forward model.

Forward modelling: north-northwest profile

The north-northwest profile P3 (Fig. 6c) was much more difficult to model than the west-southwest profile because major faults F3, F4, and F7 trend roughly perpendicular to the profile and, as for P1-P2, weakly constrained basement structure dominates the gravity signal. Geological contacts mapped in this area trend nearly perpendicular to the profile line, and surface dips in the vicinity of the Graphite uranium occurrence are steep, but elsewhere surface dips tend to be quite shallow and drill information is limited to the upper few hundred metres, so this study aims to develop deep structural constraints on major units. The 080° Thelon Fault, with some 25 km of dextral offset north of Kiggavik area (Fig. 1), likely propagated through this study area as a set of splays with smaller offsets. Some of these are labelled F3, F3a, F3b, and F7 in Figure 4a. These and more such dextral faults are interpreted by McEwan (2012) to transect the study area. They clearly offset the topographic expressions of the quartzite as seen in Figure 4a and introduce uncertainties into the model because there are few local constraints regarding their dip-slip components. For example, in addition to its strike-slip component, the Thelon Fault (Fig. 1) records some 700 m of north-side-down offset north of Kiggavik (Davis et al., 2011). In theory, the gravity model should be able to solve for this, but because the basement densities and structures are weakly defined, this becomes very uncertain; nevertheless a solution that works well here involves south-side-down dip-slip movement on a right-lateral fault at about the 18 km point on the transect. This is coincident with a distinct northeast-trending lineament on the predictive maps from source-edge detection (F4 in Fig. 3b, c, 4b) which, in turn, is roughly parallel to the klippe detachment (thrust teeth along south side) mapped in Figure 4a about 2 km northwest of the Graphite showings.

Only broad, open folds were modelled in this study due to the broad scale of the gravity signature. An open synform is inferred for the klippe at the 8 km mark (*see* P3 on Fig. 6), resting on a broad antiform in the underlying Halfway Hills assemblage. Another open synform is modelled to depth within the Pipedream metawacke, broken by the F4 fault. A broad antiform, again broken by faults with significant vertical offsets, is modelled at the south end of the transect, cresting at the 24 km mark. These folds are much more open in style compared to detailed D_2 folds mapped by B. McEwan (2012) here and elsewhere in the Tehek-Marjorie belt, but may be the regional-scale, upper crustal expression of D_2.

The Paleoproterozoic Ketyet River group rocks were modelled as for P1 and P2 in the form of thin structural sheets separated from the underlying basement by structural discontinuities. Where quartzite is present, it outcrops, here again being modelled as underlain by a thin layer of grey schist. As noted above, the scale of this modelling is too broad to identify mesoscopic folds such as identified by McEwan (2012).

The forward modelling along profile P3 provided little further information about the inferred Snow Island suite granitic intrusion. This north-northwest–south-southeast gravity transect crosses the western margin of the aeromagnetic anomaly defining the pluton, therefore in this model only a sliver of the pluton is invoked at depth, and this is cut off at its north end by the F3b fault.

The northern portion of the P3 profile (leftmost side of this profile in Fig. 6) is the least constrained part of the model, yet still provides important insights regarding horizontal tectonics. The density of the Thelon Formation sandstone is known as 2.56 g/cm^3, but at the time of modelling, no information was available for the granite that is inferred to extend beneath the Thelon Formation. The gravity signal indicates a very dense unit beneath the northwestern portion of the P3 profile because the Thelon Formation is known to be relatively low in density (Tschirhart, 2009), and granite is also typically low in density (assumed 2.56 g/cm^3). A major dense body overlain by a shallowly dipping slab of granite, in turn covered by Thelon Formation sandstone was therefore used to balance the model. Although modelling of the granite as a slab would be considered speculative based just on these data, this interpretation is consistent with the limited aeromagnetic expression of the granite, the presence

of subhorizontal felsic mylonite mapped near that area by the third author in 2011, and with evidence for thin granitic sheets and shallowly dipping structural discontinuities in the Schultz Lake intrusive complex to the west (V. Tschirhart, W.A. Morris, C.W. Jefferson, and P. Keating, unpub. data, 2012) and in the Meadowbank River area to the northeast (Thomas, 2012).

Forward modelling: summary

The generated models fit the geophysical data, are geologically feasible and are in agreement with one another (Fig. 8a, b); however, these models are only as accurate as the constraints used to create them, which are limited at best. In this area the geology is very complex and field mapping has suggested highly deformed structures. Given the available constraints the geology in these models is greatly simplified. Nonetheless, the models provide powerful first-order constraints on geological interpretations. P1 and P2 exemplify two of many different possible geological configurations that can accommodate the observed geophysical signals. Basement densities are surely the main driver for gravity profiles because the quartzite–grey schist pair is likely only a thin sheet and the nonmagnetic nature of all rock types limits the use of magnetic data for modelling.

With current data and modelling software the authors are only able to image features greater than two times the sampling space, which limits resolution of detailed structures. Interpretation is further hampered by the detailed gravity data being restricted to the two transect lines, which only allows modelling in profile. The models are also hindered by the presence of a deep-seated anomaly that may overwhelm some of the magnetic responses from near-surface source bodies. In the models, the steep-sided monolithological blocks of what are known to be layered units cannot be resolved into structurally realistic solutions, even though they do resolve geophysical signatures. Once the new data of this study and detailed mapping by McEwan (2012) are fully integrated into the next generation of regional geological maps, more data could be strategically acquired to better refine and test the models. With new sample sets and more rock properties being acquired through parallel studies (e.g. Tschirhart et al., 2012), better physical property contrasts and constraints will be available to the next generation of modellers. Considerable scope remains to fully integrate the full field data set and detailed structural geology of McEwan (2012) and other members of the GEM Uranium mapping team with these data, to further improve the models.

CONCLUSIONS

Different processing approaches integrated a multi-parameter set of geology, LANDSAT, high-resolution electromagnetic, aeromagnetic, topographic, and newly acquired high-resolution ground-gravity data. Internally consistent two-dimensional forward models and 3-D inversion models support the hypothesis of a D_1 klippe that was deformed during D_2 into upright folds and dissected by major post-D_2 strike- and dip-slip faults. Previously mapped 2.6 Ga Snow Island suite granite in the northwest part of the study area is modelled as a slab, consistent with studies to the east and west that also recognize gently dipping, thin granite bodies that developed either by intrusion as sheets and/or by structural detachment into slabs. In contrast, an inferred Snow Island suite granitic body in the southern part of the study area is modelled as a steep walled, deep-seated pluton with no near-surface details, yet a powerful overall magnetic expression.

Source-edge detection routines on gridded magnetic and electromagnetic data were used to map bulk geological contacts. The geological map by Hadlari et al. (2004) was used to provide the initial configurations and as part of a feedback process to generate models consistent with all data sets. The results of this study have been used in ongoing reinterpretation by the third author to further improve the regional map the current version of which is captured in Figure 1. In particular the structural discontinuity surface between the Ketyet River group and Woodburn Lake group is modelled as overall subhorizontal in attitude. Also, large areas previously mapped as quartzite were remapped as arkosic metawacke of the Pipedream assemblage, further clarifying the configuration of major horsts and grabens. Contacts between units within the Pipedream and Halfway Hills assemblages of the Woodburn Lake group could not be resolved from the source-edge detection routines alone because of their nonmagnetic natures in the study area, and the limited depth penetration of the EM methods.

Unconstrained 3-D inversions of the high-resolution magnetic data set using the UBC-Mag3d software helped to define regional structure and to map dyke sets and brittle faults that contribute to the development of forward models. Significant fault arrays are parallel to Mackenzie dykes (155°), Thelon dykes (~075°), and others at about 100°. It was not possible to define detailed ductile fold structures because of the nonmagnetic nature of the supracrustal units and the dominating presence of the broad, deep-seated magnetic anomaly from the inferred Snow Island pluton.

Forward models show thin crustal sheets of the Ketyet River group resting with structural discontinuity on top of the Woodburn Lake group. Steeply dipping faults offset the quartzite and schist packages of the Ketyet River group with both vertical and strike-slip displacements. Basement structures are poorly constrained, however, some detailed open F_2 folds in near surface contacts are inferred by draping EM data on topography, and major open folds are required to explain the gravity anomalies.

Given the extents of the geophysical data available and limitations on geological constraints the models presented here in most cases represent geologically possible and

geophysically consistent representations of the subsurface geology. These concepts and constraints are already improving current regional mapping.

ACKNOWLEDGMENTS

This report is based on work completed for a B.Sc. thesis by P. Tschirhart. Fieldwork and aeromagnetic data collection reported in this study were financially and logistically supported by the Northern Uranium for Canada Project under NRCan's Geomapping for Energy and Minerals Program led by C.W. Jefferson. Forum Uranium Corporation shared high-resolution aeromagnetic and electromagnetic data for the study area through collaborative exchanges with K. Wheatley and A. Williamson. Partial laboratory support for P. Tschirhart was provided by RAP salary under the GEM Program and logistical field support provided under the NRCan Volunteer Program. Laboratory and computer costs were supported by a NSERC Discovery Grant to W.A. Morris. V. Tschirhart assisted with project planning and data collection, and provided meaningful discussions about the modelling. B. McEwan (M.Sc. thesis student) and Professor K. Bethune (University of Regina) shared ideas and 2010–2011 outcrop data regarding the geology of the study area. Helicopter support was co-ordinated by Polar Continental Shelf Program through a contract with Ookpik Aviation based in Baker Lake. Critical review by P. Keating significantly improved the authors' understanding and the clarity of the manuscript.

REFERENCES

Blakely, R.J. and Simpson, R.W., 1986. Approximating edges of source bodies from magnetic or gravity anomalies; Geophysics, v. 51, p. 1494–1498. doi:10.1190/1.1442197

Chamberlain, K.R., Schmitt, A.K., Swapp, S.M., Harrison, T.M., Swoboda-Colberg, N., Bleeker, W., Peterson, T.D., Jefferson, C.W., and Khudoley, A.K., 2010. In-situ U-Pb (IN_SIMS) micro-baddeleyite dating of mafic rocks: method with examples; Precambrian Research, v. 183, p. 379–387. doi:10.1016/j.precamres.2010.05.004

Davis, W.J., Gall, Q., Jefferson, C.W., and Rainbird, R.H., 2011. Diagenetic fluorapatite in the Paleoproterozoic Thelon Basin: structural-stratigraphic context, in situ ion microprobe U-Pb ages and fluid flow history; Bulletin of the Geological Society of America, v. 123, no. 5–6, p. 1056–1073. doi:10.1130/B30163.1

Fuchs, H.D. and Hilger, W., 1989. Kiggavik (lone gull): an unconformity related uranium deposit in the Thelon Basin, Northwest Territories, Canada; Uranium Resources and Geology of North America: International Atomic Energy Agency; Technical Document, v. 500, p. 429–454.

Hadlari, T., Rainbird, R.H., and Pehrsson, S.J., 2004. Geology, Shultz Lake, Nunavut: Geological Survey of Canada, Open File 1839, scale 1:250 000. doi:10.4095/215673

Hasegawa, K., Davidson, G.I., Wollenberg, P., and Lida, Y., 1990. Geophysical exploration for unconformity-related uranium deposits in the northeastern part of the Thelon Basin, Northwest Territories, Canada; Mining Geology, v. 40, p. 83–95.

Jefferson, C.W., Thomas, D., Quirt, D., Mwenifumbo, C.J., and Brisbin, D., 2007. Empirical models for Canadian unconformity-associated uranium deposits; *in* Proceedings of Exploration 07, Exploration in the New Millennium, 5th Decennial International Conference on Mineral Exploration, Toronto, Ontario, September 9–12, 2007, p. 741–769.

Jefferson, C.W., Chorlton, L.B., Pehrsson, S.J., Peterson, T., Wollenberg, P., Scott, J., Tschirhart, V., McEwan, B., Bethune, K., Calhoun, L., White, J.C., Leblon, B., LaRocque, A., Shelat, Y., Lentz, D., Patterson, J., Riegler, T., Skulski, T., Robinson, S., Paulen, R., McClenaghan, B., Layton-Matthews, D., MacIsaac, D., Riemer, W., Stieber, C., and Tschirhart, P., 2011a. Northeast Thelon Region: Geomapping for Uranium in Nunavut; Geological Survey of Canada, Open File 6962, Power Point Presentation, 38 p. doi:10.4095/289037

Jefferson, C.W., Pehrsson, S., Peterson, T., Chorlton, L., Davis, W., Keating, P., Gandhi, S., Fortin, R., Buckle, J., Miles, W., Rainbird, R., LeCheminant, A., Tschirhart, V., Tschirhart, P., Morris, W., Scott, J., Cousens, B., McEwan, B., Bethune, K., Riemer, W., Calhoun, L., White, J., MacIsaac, D., Leblon, B., Lentz, D., LaRocque, A., Shelat, Y., Patterson, J., Enright, A., Stieber, C., and Riegler, T., 2011b. Northeast Thelon region geoscience framework - new maps and data for uranium in Nunavut; Geological Survey of Canada, Open File 6949, 1 sheet. doi:10.4095/288791

Jefferson, C.W., Pehrsson, S., Peterson, T., Wollenberg, P., Tschirhart, V., Riegler, T., McEwan, B., Tschirhart, P., Scott, J., Chorlton, L., Davis, W., Bethune, K., Riemer, W., Patterson, J., Anand, A., and Stieber, C., in press. Bedrock geology of the western Marjorie-Tehek supracrustal belt and Northeast Thelon Basin margin in parts of NTS 66A and 66B, Nunavut; Geological Survey of Canada, Open File 7241.

LeCheminant, A.N. and Heaman, L.M., 1989. Mackenzie igneous events, Canada: Middle Proterozoic hotspot magmatism associated with ocean opening; Earth and Planetary Science Letters, v. 96; Issues (National Council of State Boards of Nursing (U.S.)), v. 1–2, p. 38–48.

McEwan, B., 2012: Structural style and regional comparison of the Ketyet River group northeast of Baker Lake, Nunavut; M.Sc. thesis, The University of Regina, Regina, Saskatchewan, 127 p.

Minty, B.S., 1991. Simple micro-levelling for aeromagnetic data; Exploration Geophysics, v. 22, p. 591–592. doi:10.1071/EG991591

Pehrsson, S., Jefferson, C.W., Peterson, T., Scott, J., Chorlton, L., and Hillary, B., 2010. Basement to the Thelon Basin, Nunavut — revisited (abstract); Special Session on Geological Environments hosting Uranium Deposits, GeoCanada 2010 — Working with the Earth; Calgary, Alberta, May 10–14th, 2010, 4 p.

Peterson, T.D. and Born, P., 1994. Archean and Lower Proterozoic geology of western Dubawnt Lake, Northwest Territories; Current Research 1994-C; Geological Survey of Canada, p. 157–164.

Peterson, T., Pehrsson, S., Jefferson, C., Scott, J., and Rainbird, R., 2010. The Dubawnt Supergroup, Canada: a LIP with a LISP; December 2010 LIP of the month; http://www.largeigneousprovinces.org/lom.html [accessed January 12, 2012], 32 p.

Pilkington, M. and Keating, P.B., 2004. Contact mapping from gridded magnetic data – a comparison of techniques; Exploration Geophysics, v. 35, p. 306–311. doi:10.1071/EG04306

Rainbird, R.H., Hadlari, T., Aspler, L.B., Donaldson, J.A., LeCheminant, A.N., and Peterson, T.D., 2003. Sequence stratigraphy and evolution of the Paleoproterozoic intracontinental Baker Lake and Thelon basins, western Churchill Province, Nunavut, Canada; Precambrian Research, v. 125, p. 21–53. doi:10.1016/S0301-9268(03)00076-7

Rainbird, R.H., Davis, W.J., Pehrsson, S.J., Wodicka, N., Rayner, N., and Skulski, T., 2010. Early Paleoproterozoic supracrustal assemblages of the Rae domain, Nunavut, Canada: intracratonic basin development during supercontinent break-up and assembly; Precambrian Research, v. 181, p. 167–186. doi:10.1016/j.precamres.2010.06.005

Renac, C., Kyser, T.K., Durocher, K., Dreaver, G., and O'Connor, T., 2002. Comparison of diagenetic fluids in the Proterozoic Thelon and Athabasca Basins, Canada: implications for protracted fluid histories in stable intracratonic basins; Canadian Journal of Earth Sciences, v. 39, p. 113–132. doi:10.1139/e01-077

Scott, J.M.J., 2012: Paleoproterozoic (1.75 Ga) granitoid rocks and uranium mineralization in the Baker Lake–Thelon Basin region, Nunavut; Master's thesis, Department of Earth Sciences, Carleton University, Ottawa, Ontario, 136 p.

Scott, J., Peterson, T.D., Jefferson, C.W., and Cousens, B., 2010. (extended abstract): Proterozoic (1.85–1.7 Ga) granitoid rocks and uranium in the Baker Lake–Thelon Basin region, Nunavut; GeoCanada 2010, Calgary, Alberta, May 10–14, 4 p.

Spicer, B., 2010. Geologically constrained geophysical modeling of magnetics and gravity — the Baie Verte Peninsula, Newfoundland; M.Sc. thesis, McMaster University, Hamilton, Ontario, 161 p.

Thomas, M.D., 2012. Shallow crustal structure in the Meadowbank River–Tehek Lake area: insights from gravity and magnetic modelling; Geological Survey of Canada, Open File 7308, 42 p. doi:10.4095/292157

Thomas, M.D. and Wood, G., 2007. Geological significance of gravity anomalies in the area of McArthur River uranium deposit, Athabasca Basin, Saskatchewan; *in* EXTECH IV: Geology and Uranium Exploration TECHnology of the Proterozoic Athabasca Basin, Saskatchewan and Alberta, (ed.) C.W. Jefferson and G. Delaney; Geological Survey of Canada, Bulletin 588, p. 441–464. doi:10.4095/223742

Tschirhart, V., 2009. 3D geophysical modeling of the northeastern Thelon Basin, Nunavut; B.Sc. thesis, McMaster University, Hamilton, Ontario, 29 p.

Tschirhart, V., Morris, W.A., and Oneschuk, D., 2011a. Geophysical series, geophysical compilation project, Thelon Basin, Nunavut, NTS 66A, B, and parts of 65N, O, P, 66C, F, G and H; Geological Survey of Canada, Open File 6944, 1 sheet. doi:10.4095/288806

Tschirhart, V., Morris, W.A., Ugalde, H., and Jefferson, C.W., 2011b. Preliminary 3D geophysical modelling of the Aberdeen sub-basin, northeast Thelon Basin region, Nunavut; Geological Survey of Canada, Current Research 2011-4, 12 p. doi:10.4095/287165

Tschirhart, V., Morris, W.A., Jefferson, C.W., Keating, P., White, J.C., and Calhoun, L., 2012. 3D geophysical inversions of the north-east Amer Belt and their relationship to the geologic structure; Geophysical Prospecting. doi:10.1111/j.1365-2478.2012.01098.x

Tschirhart, V., Morris, W.A., and Jefferson, C.W., in press: Framework modeling of granitoid vs supracrustal basement to the northeast Thelon Basin around the Kiggavik uranium camp, Nunavut; Canadian Journal of Earth Sciences.

Williams, N.C., 2008. Geologically-constrained UBC-GIF gravity and magnetic inversions with examples from the Agnew-Wiluna Greenstone Belt, Western Australia; Ph.D. thesis, University of British Columbia, Vancouver, British Columbia, 479 p.

Zaleski, E., Pehrsson, S., Duke, N., Davis, W.J., L'Heureux, R., Greiner, E., and Kerswill, J.A., 2000. Quartzite sequences and their relationships, Woodburn Lake group, western Churchill Province, Nunavut; Geological Survey of Canada, Current Research 2000-C7, 10 p. doi:10.4095/211098

Geological Survey of Canada Project EGM 007